Arabian Journal of Chemistry (2016) **xxx**, xxx–xxx

King Saud University

Arabian Journal of Chemistry

www.ksu.edu.sa
www.sciencedirect.com

ORIGINAL ARTICLE

Spectroscopic (IR, Raman, NMR), thermal and theoretical (DFT) study of alkali metal dipicolinates (2,6) and quinolinates (2,3)

G. Świderski [a,*], H. Lewandowska [c], R. Świsłocka [a], S. Wojtulewski [b], L. Siergiejczyk [b], A.Z. Wilczewska [b], I. Misztalewska [b]

[a] *Division of Chemistry, Bialystok University of Technology, Wiejska 45E Street, 15-351 Bialystok, Poland*
[b] *Institut of Chemistry, University of Bialystok, Ciolkowskiego Street 1K, 15-245 Bialystok, Poland*
[c] *Institute of Nuclear Chemistry and Technology, Centre for Radiobiology and Biological Dosimetry, Dorodna 16, 03-195 Warsaw, Poland*

Received 7 March 2016; accepted 16 June 2016

KEYWORDS

Dipicolinic acid;
Quinolinic acid;
Pyridinedicarboxylic acid;
Dipicolinates;
Quinolinates;
Alkali metal salts

Abstract In the presented work the thermal, theoretical (DFT) and spectroscopic (IR, Raman, NMR) properties of alkali metal complexes with quinolinic acid (2,3-pyridinedicarboxylic acid) and dipicolinic acid (2,6-pyridinedicarboxylic acid) were studied. The IR and Raman spectra were registered and analyzed in the range of 400–4000 cm^{-1}. ^{1}H NMR and ^{13}C NMR spectra of analyzed compounds have been registered and assigned. The electronic charge distribution for the studied acids and their salts with lithium, sodium and potassium was calculated. All the calculations were done in the frame of density functional theory (DFT) using 6-311 + + G(d,p) basis set. The thermal decomposition of the analyzed compounds was done.

1. Introduction

In this paper we decided to focus on the physicochemical properties and thermal decomposition of the quinolinic acid (2,3-pyridinedicarboxylic, 2,3-PDA) and dipicolinic acid (2,6-pyridinedicarboxylic, 2,6-PDA). These acids are two of the six pyridinedicarboxylic acid isomers. They are ligands of high biological importance. Quinolinic acid is one of the final products of tryptophan transformation in the kynurenine pathway (Fig. 1). The kynurenine pathway is a major route of tryptophan catabolism, resulting in the production of nicotinamide adenine dinucleotide (NAD +) and several neuroactive intermediates (Fig. 1) (Heyes et al., 1992). In the metabolic pathway there are also produced other pyridinecarboxylic acids (picolinic acid and nicotinic acid, studied in our earlier works) that play important roles in the body. In pathological conditions, the elevated concentration of quinolinic acid causes strong neurotoxicity (Pérez-De La Cruz et al., 2007). Quinolinic acid neurotoxicity is supposed to be caused partly by the over-excitation of the N-methyl-D-aspartate (NMDA) receptor and partly by elevated levels of cytotoxic reactive oxygen species (ROS) in the brain tissue (Kubicova et al., 2015). There is accumulating evidence that quinolinic acid is involved

* Corresponding author. Fax: +48 5 746 95 59.
E-mail address: swider30@gmail.com (G. Świderski).
Peer review under responsibility of King Saud University.

Production and hosting by Elsevier

http://dx.doi.org/10.1016/j.arabjc.2016.06.011
1878-5352 © 2016 The Authors. Production and hosting by Elsevier B.V. on behalf of King Saud University.

Please cite this article in press as: Świderski, G. et al., Spectroscopic (IR, Raman, NMR), thermal and theoretical (DFT) study of alkali metal dipicolinates (2,6) and quinolinates (2,3). Arabian Journal of Chemistry (2016), http://dx.doi.org/10.1016/j.arabjc.2016.06.011

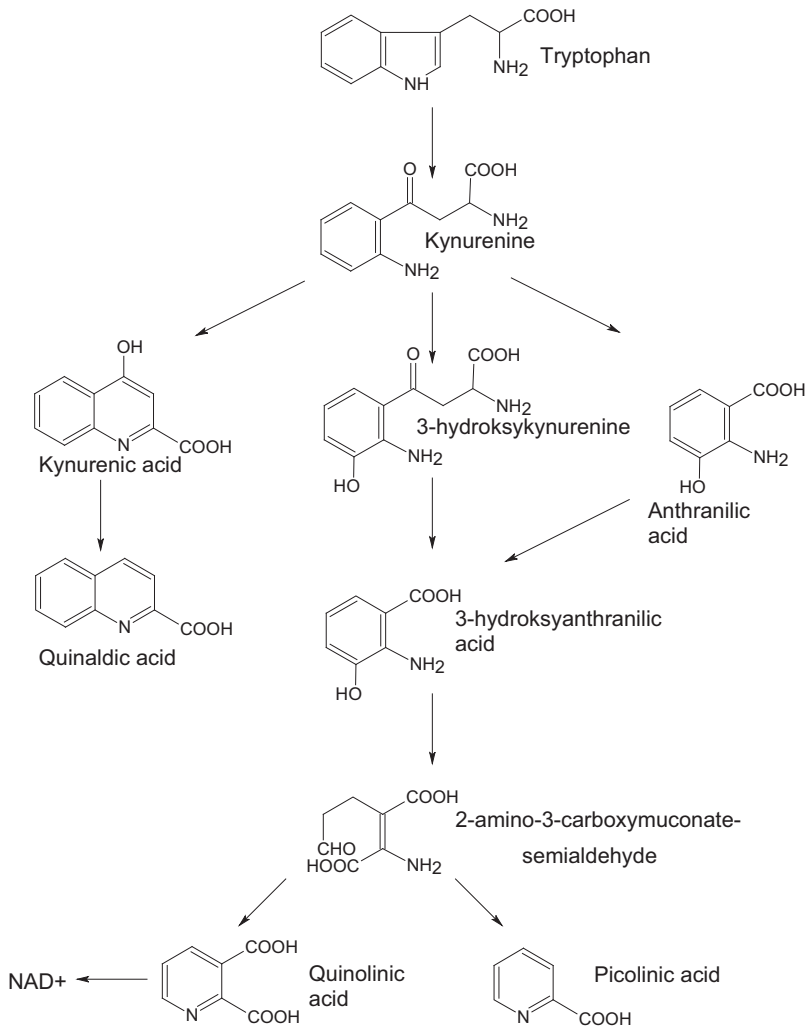

Figure 1 Kynurenine pathway (Chen et al., 2011).

in the neurotoxicity associated with several inflammatory brain diseases such as Alzheimer's (Guillemin and Brew, 2002; Guillemin et al., 2003, 2005; Rahman et al., 2009), Parkinson's (Zinger et al., 2011), motor neuron (Chen et al., 2010), Huntington's diseases (Stoy et al., 2005; Bruyn and Stoof, 1990) and multiple sclerosis (Hartai et al., 2005; Lim et al., 2010). Dipicolinic acid and its salts are important components of the bacterial spores. These substances increase the resistance of the spores to UV radiation (Powell and Strange, 1953; Slieman and Nicholson, 2001) and improve the stability of bacterial spores (the aerobic *Bacillus* and anaerobic *Clostridium*).

Pyridinecarboxylic and dipyridinecarboxylic acids are potent natural chelators. The presence of nitrogen in the pyridine ring can create a stable connection chelate of N, O-metal coordination of different types. In our previous work we studied complexes of some pyridinecarboxylic acid (nicotinic, isonicotinic and picolinic) isomers with various metals. We analyzed the effect of metal on the change in the electronic charge distribution under the influence of ligands complexing different metals, and antimicrobial properties of complexes. Examined were, *inter alia*, pyridinecarboxylic acid salts of alkali metals (lithium, sodium, potassium, rubidium and cesium). Alkali metals destabilized the electronic system of the aromatic ring in the analyzed acids (Lewandowski et al., 2005; Koczoń et al., 2006; Świderski et al., 2006; Kalinowska et al., 2007). It was shown that the degree of destabilization depended on the type of metal, and the position of the nitrogen in the pyridine ring relative to the carboxyl groups. Spectroscopic studies (FT-IR, FT-Raman, NMR) and theoretical calculations (electron charge distribution) showed that the alkali metal cations disrupted the electronic system of pyridinecarboxylic acid, and the perturbation increased in the following order: Li → Na → K → Rb → Cs (Lewandowski et al., 2005; Koczoń et al., 2006; Świderski et al., 2006; Kalinowska et al., 2007). Based on these studies, we have found that alkali metals have less impact on the electronic system of picolinic and nicotinic than of isonicotinic acid. Alkali metals to the highest degree interfered with the aromatic system of nicotinic acid. In the present study we compare the effect of alkali metals on the electron system of two other ligands – pyridinecarboxylic acids (dipicolinic and chinolinic acids); the thermogravimetric properties of the salts are tested (see Fig. 2).

2. Material and methods

2.1. Sample preparation

The alkali metal salts of 2,3-pyridinedicarboxylic and 2,6-pyridinedicarboxylic acids were prepared by dissolving appropriate weighed amount of particular acids in aqueous solution of alkali metal hydroxides in a stoichiometric ratio ligand:metal – 1:2. 0.1 mol of 2,3-pyridinedicarboxylic acid,

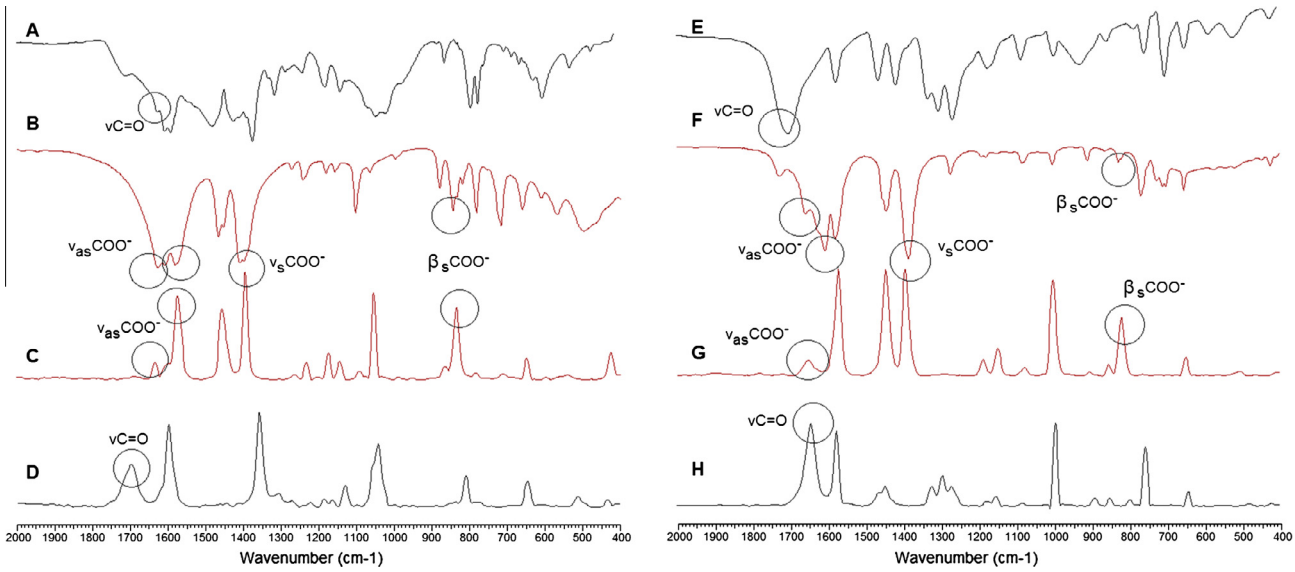

Figure 2 FTIR spectra A, B, E, F and Raman spectra (C, D, G, H) for 2,3-pyridinedicarboxylic acid (A, D) and sodium salt (B, C); 2,6-pyridinedicarboxylic acid (E, H) and sodium salts (F, G).

was added to 20 mL of the previously prepared metal hydroxide solutions having a concentration of 0.1 M. The synthesis of alkali metal salts of 2,6-pyridinedicarboxylic acid was performed in a similar manner. The mixtures were heated on a steam bath with stirring until the acid dissolved in sodium hydroxide. Then, water was evaporated on a water bath and dried in an oven at 70 °C for 24 h. All chemicals were purchased from Sigma–Aldrich.

2.2. Measurement and calculation

The FT-IR spectra were recorded with an Alfa (Bruker) spectrometer within the range of 400–4000 cm^{-1}. Samples in the solid state were measured in KBr matrix pellets and in ATR technique. FT-Raman spectra of solid samples were recorded in the range of 400–4000 cm^{-1} with a MultiRam (Bruker) spectrometer. The resolution of the spectrometer was 1 cm^{-1}. The ^{1}H and ^{13}C NMR spectra of D_2O solution of studied compounds were recorded with a Bruker Avance II 400 MHz unit at room temperature. TMS was used as an internal reference. To calculate optimized geometrical structures of 2,3-, 2,6-pyridinedicarboxylic acid and lithium, sodium and potassium salts quantum–mechanical methods were used: density functional (DFT) hybrid method B3LYP with non-local correlation provided by Lee–Young–Parr expression. All calculations were carried out with functional base 6-311 + + G(d,p). Calculations were performed using the Gaussian 09 (Frisch et al., 2009) package. Experimental spectra were interpreted in terms of DFT method calculations in B3LYP/6-311 + + G(d,p) level and literature data (McCann and Laane, 2008; Karabacak et al., 2015). Theoretical wave numbers were scaled according to the formula: $\nu_{scaled} = 0.98 \cdot \nu_{calculated}$ for B3LYP/6-311 + + G(d,p) level method (Rode et al., 2001). Chemical shifts (δi) were calculated by subtracting the appropriate isotopic part of the shielding tensor (σi) from that of TMS (σ_{TMS}): $\delta i = \sigma_{TMS} - \sigma i$ (ppm). The isotropic shielding constants for TMS calculated using the DFT method at the same level of theory were equal to 31.8201 ppm and 182.4485 ppm for the ^{1}H nuclei and the ^{13}C nuclei, respectively. The products of dehydration and decomposition processes were determined from the TG curves. Thermogravimetric analysis (TGA) was performed on a Mettler Toledo Star TGA/DSC1 unit. Argon was used as a purge gas (20 ml min^{-1}). Samples between 2 and 4 mg were placed in aluminum pans and heated from 50 °C to 900 °C with a heating rate of 10 °C/min.

3. Results and discussion

3.1. IR and Raman Spectra

The wave numbers, intensities and assignments of the bands occurring in the IR (KBr and ATR) and Raman spectra of 2,3-pyridinedicarboxylates are presented in Table 1 and 2,6-pyridinedicarboxylates are presented in Table 2. The spectral assignments were done on the basis of the literature data (McCann and Laane, 2008; Karabacak et al., 2015) and calculated IR wave numbers of studied compounds. Theoretical spectra for acids and lithium, sodium, potassium salts were calculated by DFT/B3LYP method on 6-311 + + G^{**} basis. Calculated normal vibrations were characterized by computer animation. A good correlation between experimental and theoretical IR and Raman spectra was noted. The correlation coefficients for the IR spectra are higher than 0.990. Normal vibrations of the aromatic ring were given by Varsanyi (1973). The changes of intensities and wave numbers of the bands of the aromatic system in the case of salts were discussed, in comparison with the free ligands. Substitution of the metal ion in the two groups of carboxylic acids results in the disappearance of the characteristic vibration of the carboxyl group, such as v(C═O) in 2,3-PDA present at 1707, 1622 cm^{-1} in the IR_{KBr} spectrum, 1706 cm^{-1} in the IR_{ATR} spectrum, 1698 cm^{-1} in Raman, in the 2,6-PDA acid present at 1701 cm^{-1} in IR_{KBr}, 1693 and 1634 cm^{-1} in IR_{ATR} and 1644 cm^{-1} in Raman; v(C—O) in 2,3-PDA present at 1307 cm^{-1} in IR_{KBr}, 1307 cm^{-1} in IR_{ATR}, 1309 cm^{-1} in

Table 1 Wave numbers (cm^{-1}), intensities and assignments of bands occurring in the IR (KBr, ATR and DFT) and Raman spectra of 2,3-pyridinedicarboxylic acid and lithium, sodium, potassium, rubidium and cesium 2,3-pyridinedicarboxylates.

2,3-pyridinedicarboxylic acid					2,3-pyridinedicarboxylate															Assignments	
					Lithium					Sodium					Potassium						
IR KBr	IR ATR	Raman	IR theoret	Inten	IR KBr	IR ATR	Raman	IR theore	Inten	IR KBr	IR ATR	Raman	IR theor	Inten	IR KBr	IR ATR	Raman	IR theoret	Inten		
3441 s			3627	112.96																ν(OH)	
		3170 vw																		ν(OH)	
3104 s	3104 s	3104 s	3101	4.97				3104	5.26				3086	18.95			3102 w	3101	8.24	$\nu(CH)_{ar}$	2
		3087 vs	3089	4.02			3079 vs	3084	10.71			3060 vs	3071	11.56			3079 s	3073	22.55	$\nu(CH)_{ar}$	7a
			3059	11.13			3029 vw	3047	17.89				3040	22.07				3033	27.87	$\nu(CH)_{ar}$	7b
1707 m	1706 m	1698 w	1757	330.13																ν(C═O)	
1622 s			1735	383.11																ν(C═O)	
					1626 vs	1623 s	1623 vw	1549	477.86	1593 vs	1592 s	1633 w	1555	290.22	1602 vs	1590 vs	1627 vw	1558	486.33	$\nu_{as}COO^-$	
1602 vs	1600 s	1600 m																		$\nu(CH)_{ar}$. $\nu(CN)_{ar}$. β $(CH)_{ar}$	
					1579 vs	1573 vs	1581 m	1485	301.13	1563 vs	1562 vs	1573 s	1528	65.19	1558 vs		1581 s	1491	357.42	$\nu_{as}COO^-$	
1586 vs	1583 m																			$\nu(CH)_{ar}$. $\nu(CN)_{ar}$	
1474 s	1471 s		1573	56.71	1464 s	1464 s	1469 m	1574	81.22	–		1457 s	1569	74.49	–			1571	101.87	$\nu(CC)_{ar}$. $\nu(CN)_{ar}$	8b
		1446 vw	1432	12.09	1452 s	1452 s		1546	146.8	1456 m	1449 m		1543	290.41	1457 s	1453 s	1451 w	1546	132.07	$\nu(CC)_{ar}$. $\nu(CN)_{ar}$	8a
1418 s	1416 s		1423	24.63				1421	109.15				1429	15.86				1413	29.74	$\nu(CC)_{ar}$. $\nu(CN)_{ar}$. β $(CH)_{ar}$	3
			1328	40.42				1372	257.10				1369	297.10				1363	214.98	$\nu(CC)_{ar}$. $\nu(CN)_{ar}$. β $(CH)_{ar}$	19b
					1408 vs	1403 s	1409 w	1348	303.62	1394 vs	1391 vs	1395 vs	1338	219.33	1385 vs	1379 vs	1388 vs	1343	429.55	$\nu_{sym}COO^-$	
					1398 vs	1395 vs	1393 m	–	–	–			–	–	–			–	–	$\nu_{sym}COO^-$	
1367 vs	1364 vs	1359 m	1324	186.58																β(OH)	
1307 s	1307 m	1309 vw																		β(OH)	
1279 m		1274 vw	1251	1.67	1270 w	1269 w	1274 vw	1244	11.13	1266 vw	1266 vw	1266 vw	1245	8.61	1248 vw		1233 w	1233	9.69	$\nu(CC)_{ar}$. $\nu(CN)_{ar}$. β $(CH)_{ar}$	15
1234 m	1235 w	1224 vw	1231	11.7	1241 w	1242 w	1241 vw	1225	7.98	1235 w	1236 w	1235 w	1223	23.51	1231 w	1231 w		1224	3.23	$\nu(CC)_{ar}$. $\nu(CN)_{ar}$. β $(CH)_{ar}$	14
1173 m	1174 m	1187 vw	1189	157.63	1180 w		1183 w	1158	17.58	1175 w		1177 w	1154	28.98	1175 w		1176 w	1150	24.12	$\beta(CH)_{ar}$	18b
		1166 vw	1159	38.3			1152 vw													β(OH)	

Table 1 (*continued*)

2,3-pyridinedicarboxylic acid					2,3-pyridinedicarboxylate															
					Lithium					Sodium					Potassium					Assignments	
IR KBr	IR ATR	Raman	IR theoret	Inten	IR KBr	IR ATR	Raman	IR theore	Inten	IR KBr	IR ATR	Raman	IR theor	Inten	IR KBr	IR ATR	Raman	IR theoret	Inten		
1132 m	1131 m	1133 w	1107	216.49				1128	17.36	1151 w		1147 w	1125	1.37	1156 w	1147 w	1154 w	1125	15.46	$\beta(CH)_{ar}$	9b
1115 m			1100	135.72	1102 m	1102 m	1102 vw	1071	8.27	1096 m	1095 m	1095 vw	1070	17.92	1089 m	1088 w	1093 w	1065	15.34	$\beta(CH)_{ar}$	9a
			1057	54.44	1064 w		1064 m	1039	2.36	1059 vw		1058 s	1040	1.76	1059 w		1068 s	1039	1.26	$\beta(CH)_{ar}$	18a
1038 s	1037 s	1044 m	1036	8.02								1039 vw								Ring def	
1011 s	1005 s		980	1.12	996 vw			972	0.51	996 vw		992 vw	957	0.73			985 vw	971	0.74	$\Phi(CC)_{ar}$. $\gamma(CH)_{ar}$	5
970 m	967 m	975 vw	954	0.21			965 vw	953	0.01	953 vw		956 vw	–	–			963 vw	944	0.07	$\Phi(CC)_{ar}$. $\gamma(CH)_{ar}$	10b
874 w					878 m	879 m	880 vw	869	37.24	871 w	871 w	871 w	851	22.84	868 w	864 w	867 vw	–	–	$\alpha(CCC)$	12
853 m	853 m	840 vw	821	1.29																$\gamma(CH)_{ar}$	11
					843 m	843 m	846 m	848	8.58	836 m	834 m	840 s	831	7.48	834 m	827 m	834 m	849	18.58	$\beta_{sym}COO^-$	
		813 w	809	6.07	819 w			823	0.10	814 w	804 w		816	9.25			811 w	819	49.54	Ring def	
782 s	779 s	780 vw	789	35.55	782 m	782 m	784 vw	776	44.22	785 m	785 m	788 vw	778	33.47	790 m	782 m		778	38.74	$\gamma(CH)_{ar}$	
763 s	760 vs		759	80.6	751 m			741	16.83	754 vw	758 w		721	29.99	756 w	753 w	757 vw	741	16.24	Ring def	
749 m			728	22.01																$\gamma(CH)_{ar}$	
694 w	694 w		628	36.62	717 s	715 s	722 vw	720	45.49	717 s	715 s	717 vw	707	25.13	721 m	711 m	720 vw	708	37.17	$\alpha(CCC)$	6b
673 w	673 w									668 w					667 w	670 w				$\gamma(CH)_{ar}$	
653 m	653 w	651 w	615	35.19	660 m	660 m	661 w	639	48.62	653 w	653 w	655 w	636	13.40	650 m	646 m	651 w	632	11.52	$\alpha(CCC)$	6a
640 m	642 m																			$\gamma(CH)_{ar}$	
616 m		618 vw			610 m		614 vw	601	180.17	605 w	605 w	605 vw								Ring def	
591 s			580	65.88																$\gamma(CH)_{ar}$	
		576 vw	557	12.58	568 m		564 vw	560	3.67	574 w		547 vw	548	3.30	579 m		584 vw	564	3.04	$\Phi(CC)_{ar}$. $\gamma(CH)_{ar}$	4
518 m		518 vw	499	20.43																$\beta(OH)$	
					497 s			508	2.70				–	–				509	15.84	$\beta_{as}COO^-$	
438 w		439 vw	402	0.98			445 vw	434	98.19	436 w		433 w	451	46.64	422 w		423 w	443	55.70	$\Phi(CC)_{ar}$	16b

Rubidium 2,3-pyridinedicarboxylate			Cesium 2,3-pyridinedicarboxylate			Assignments	
IR KBr	IR ATR	Raman	IR KBr	IR ATR	Raman		
		3060 vs			3054 vs	$\nu(CH)_{ar}$	7b
1596 vs	1590 vs		1595 vs	1587 vs		$\nu_{as}COO^-$	
1575 vs		1571 m	1575 vs		1573 s	$\nu_{as}COO^-$	
1454 m	1450 m	1453 m	1453 m	1447 m	1442 m	$\nu(CC)_{ar}$, $\nu(CN)_{ar}$	8a
1382 vs	1376 vs	1393 m	1382 vs	1372 vs	1386 vs	$\nu_{sym}COO^-$	
1265 vw		1266 vw	1263 vw		1257 vw	$\nu(CC)_{ar}$, $\nu(CN)_{ar}$, $\beta(CH)_{ar}$	15
1229 w		1231 vw	1229 vw	1229 w	1226 w	$\nu(CC)_{ar}$, $\nu(CN)_{ar}$, $\beta(CH)_{ar}$	14
1178 w	1173 w	1176 w	1178 w	1173 w	1174 m	$\beta(CH)_{ar}$	18b
1149 w	1144 w	1145 w	1149 w	1143 w	1145 w	$\beta(CH)_{ar}$	9b
1093 m	1086 w	1085 vw	1092 w	1083 w	1085 w	$\beta(CH)_{ar}$	9a
1058 w		1052 s	1058 vw		1052 vs	$\beta(CH)_{ar}$	18a
		1021 vw	1031			Ring def	

(*continued on next page*)

Table 1 (*continued*)

Rubidium 2,3-pyridinedicarboxylate			Cesium 2,3-pyridinedicarboxylate			Assignments	
IR KBr	IR ATR	Raman	IR KBr	IR ATR	Raman		
868 m	864 m		867 w	861 w	859 w		
831 m	826 m	828 m	830 m	823 m	823 s	$\beta_{sym}COO^-$	
786 m	783 m		786 m	780 m		Ring def	
		751 vw					
717 m	708 m	715 vw	717 m	709 m	713 vw	α(CCC)	6b
		674 vw	668 m			$\gamma(CH)_{ar}$	
651 m	644 m	647 w	651 m	643 m	645 w	α(CCC)	6a
617 m						Ring def	
581 m		583 vw	581 m		580 vw	$\Phi(CC)_{ar}$, $\gamma(CH)_{ar}$	4
426 m		412 w	425 w		412 m	$\Phi(CC)_a$	16b

Raman, in 2,6-PDA present at 1328 cm^{-1} in IR_{KBr}, 1331 cm^{-1} in IR_{ATR} and 1328 cm^{-1} in Raman. Vibration bands of the hydroxyl group i.e. ν(OH), β(OH) and γ(OH) disappear as well. The disappearance of the bands characteristic of the carboxyl group indicates that the two carboxyl groups are being substituted by the metal ion. In the spectra of salts there appear bands assigned to vibrations of the carboxylate anion (the metal to ligand ratio was 2:1). In the alkali metal salts with 2,3-PDA these new vibrations give characteristic wide and intense two bands responsible for the $\nu_{as}(COO^-)$ (1626–1590 and 1579–1575 cm^{-1} in IR_{KBr} spectra, 1623–1587 and 1573–1562 cm^{-1} in IR_{ATR}, 1633–1623 and 1581–1571 cm^{-1} Raman spectra) and $\nu_{sym}(COO^-)$ (1408–1382 cm^{-1} in IR_{KBr} spectra, 1403–1372 cm^{-1} in IR_{ATR}, 1409–1386 cm^{-1} in Raman spectra) stretching of the carboxylic anion. The bands assigned to the symmetric in-plane deformation of the carboxylic anion (β_{sym}: 843–830 cm^{-1} IR_{KBr} spectra, 843–823 cm^{-1} IR_{ATR}, 846–823 cm^{-1} Raman spectra) and asymmetric in-plane deformation of the carboxylic anion (β_{as}, observed only in the case of lithium salt, 497 IR_{KBr}). Bands derived from the carboxylate anion vibration in the spectra of the alkali metal salt of the 2,6-PDA occur at somewhat higher wave numbers than it is the case of the spectra of 2,3-PDA salts. In the alkali metal salts with 2,6-PDA these vibrations gave characteristic wide and intense two bands responsible for the $\nu_{as}(COO^-)$ (1656–1646 and 1612–1609 cm^{-1} in IR_{KBr} spectra, 1658–1631 and 1614–1669 cm^{-1} in IR_{ATR}, 1665–1636 and 1619 cm^{-1} in Raman spectra) and $\nu_{sym}(COO^-)$ (1384–1378 cm^{-1} in IR_{KBr} spectra, 1385–1365 cm^{-1} in IR_{ATR}, 1397–1386 cm^{-1} in Raman spectra) stretching of the carboxylic anion. The bands assigned to the symmetric in-plane deformation of the carboxylic anion, β_{sym} occur at 827–816 cm^{-1} in IR_{KBr}, 826–813 cm^{-1} in IR_{ATR}, 826–815 cm^{-1} in Raman. Asymmetric in-plane deformation of the carboxylic anion was not observed in the 2,6-PDA salts.

The bands derived from aromatic ring vibrations of the studied acids and their salts with alkali metals are present in the entire spectral range. As compared to the spectra of acids, in the spectra of the salts a decrease in the wave numbers can be seen and the intensity of vibrations of the aromatic system is reduced. A number of bands present in the acid spectra disappear in the salts upon the metal ion substitution at the carboxyl group and as well some additional bands emerge that aren't present in the spectra of the ligands. Based on the comparison of the wave numbers and intensities of the aromatic ring vibration bands (vibration of C—C and C—H bonds in the aromatic ring) in the ligand and salts, some conclusions can be drawn on the influence of metal on a disturbance or stabilization of the aromatic ring. The disturbance of this system is indicated by the reduction in the number and intensity of the bands derived from the aromatic system vibrations and/or their shift toward lower wave numbers in the IR and Raman spectra of the complexes compared to the spectrum of a given acid; this is due to the reduction in the force constants and polarization of C—C and C—H bonds in the ring. It was observed that in the IR and Raman spectra more bands present on the ligand disappear in the case of 2,3-PDA salts than it is in the case of 2,6-PDA salts. In addition, salts of 2,6-PDA reveal more new ligand bands than 2,3-PDA salts. The wave numbers of some bands present in the spectra of the salts tested decrease in the series Li → Na → K → Rb → Cs. These changes are not regular as it is observed for the spectra of alkali metal salts with monocarboxy-pyridinecarboxylic acids.

Table 2 Wave numbers (cm^{-1}), intensities and assignments of bands occurring in the IR (KBr, ATR and DFT) and Raman spectra of 2,6-pyridinedicarboxylic acid and lithium, sodium, potassium, rubidium and cesium 2,6-pyridinedicarboxylates.

2,6-pyridinedicarboxylic acid					2,6-pyridinedicarboxylate															Assignments	
					Lithium					Sodium					Potassium						
IR KBr	IR ATR	Raman	IR theor	Inten	IR KBr	IR ATR	Raman	IR theor	Inten	IR KBr	IR ATR	Raman	IR theore	Inten	IR KBr	IR ATR	Raman	IR theoret	Inten		
			3638	90.98																ν(OH)	
3430 m			3638	109.64																ν(OH)	
		3148 w					3141 vw					3141 vw								$\nu(CH)_{ar}$	20a
		3098 s	3109	0.86				3109	3.11				3108	5.22				3106	6.44	$\nu(CH)_{ar}$	2
3068 s		3071 s	3106	1.27			3079 vs	3107	0.11			3075 s	3106	0.01	3063 w		3079 s	3104	0.09	$\nu(CH)_{ar}$	7b
2998 s		3008 vw	3080	4.90			3021 vw	3066	12.70			3006 w	3059	18.53			3000 vw	3053	22.75	$\nu(CH)_{ar}$	13
1701 vs	1693 vs		1726	136.17																ν(C═O)	
	1634 s	1644 vs	1721	557.03																ν(C═O)	
					1646 vs	1658 m	1665 w	1516	734.47	1656 m		1652 w	1527	113.97	1648 s		1650 vw	1533	93.59	$\nu_{as}COO^-$	
					1609 s	1614 s		1516	73.10	1605 vs	1614 s		1527	697.24	1612 vs	1609 s	1619 vw	1532	593.41	$\nu_{as}COO^-$	
			1566	4.26	1588 s	1580 s		1568	84.89				1568	143.58				1569	188.60	$\nu(CC)_{ar.}$ $\nu(CN)_{ar}$	8a
1573 s	1575 s	1577 vs	1561	1.96	1573 s		1573 s	1562	4.74	1578 s	1576 s	1573 vs	1561	3.01	1576 s	1576 s	1571 s	1561	4.56	$\nu(CC)_{ar.}$ $\nu(CN)_{ar}$	8b
1462 m	1463 m	1461 w	1434	0.01	1460 m	1463 m	1455 m	1419	54.03	1488 vw			1414	6.92				1412	4.22	$\nu(CC)_{ar.}$ $\nu(CN)_{ar.}$ β $(CH)_{ar}$	19a
	1456 w	1447 w	1408	19.09	1443 s	1447 m				1443 m	1442 m	1447 vs	1406	31.57	1433 m	1430 m	1436 s	1402	40.45	$\nu(CC)_{ar.}$ $\nu(CN)_{ar.}$ β $(CH)_{ar}$	19b
1415 s	1416 s		1356	198.76																β(OH)	
					1384 vs	1385 vs		1361	5.60	1384 vs	1382 vs	1397 vs	1349	17.15	1379 vs	1375 vs	1392 vs	1345	32.88	$\nu_{sym}COO^-$	
								1365	698.38				1344	667.96				1337	778.76	$\nu_{sym}COO^-$	
1328 s	1331 s	1324 w																		β(OH)	
1300 s	1299 vs	1297 m	1330	61.43								1295 vw					1299 vw			$\nu(CC)_{ar.}$ $\nu(CN)_{ar.}$ β $(CH)_{ar}$	3
1263 s	1263 vs	1272 w	1277	6.41	1276 m	1273 m	1280 vw	1263	28.43	1273 w	1275 w		1257	30.63	1266 w	1267 m		1254	36.67	$\nu(CC)_{ar.}$ $\nu(CN)_{ar.}$ β $(CH)_{ar}$	15
			1193	197.53																β(OH) + def ring	
1171 m	1178 m	1179 vw			1188 w			1159	5.54	1191 vw	1190 w	1191 w	1156	6.54	1184 w	1184 w	1189 w	1155	6.81	$\beta(CH)_{ar}$	
	1164 s	1154 w	1136	1.04	1153 w		1152 w	1128	1.51	1151 vw		1152 w	1126	2.08	1147 w		1149 m	1123	2.01	$\beta(CH)_{ar}$	18b
			1106	260.87																ν(C—O)	
			1095	41.17																β(OH)	
1082 m	1082 m	1085 vw			1088 w	1082 w	1083 vw	1061	22.98	1083 w	1081 w	1081 vw	1058	23.21	1072 w	1075 w	1075 vw	1056	23.71	$\beta(CH)_{ar}$	18a
			995	0.34	1013 m	1013 w	1015 s	994	0.53	1003 w	1005 w	1006 s	990	0.74	1000 w	1003 w	1004 vs	989	0.75	$\Phi(CC)_{ar.}$ $\gamma(CH)_{ar}$	17b

(*continued on next page*)

Table 2 (*continued*)

2,6-pyridinedicarboxylic acid					2,6-pyridinedicarboxylate																
					Lithium					Sodium					Potassium					Assignments	
IR KBr	IR ATR	Raman	IR theor	Inten	IR KBr	IR ATR	Raman	IR theor	Inten	IR KBr	IR ATR	Raman	IR theore	Inten	IR KBr	IR ATR	Raman	IR theoret	Inten		
994 m	997 m	998 vs	981	9.14				978	4.03				977	3.56				977	3.15	α(CCC)	12
	912 m		940	0.01	915 w		919 vw	942	0.01	909 w	911 w	909 vw	940	0.01	902 w	906 w	906 vw	936	0.01	$\Phi(CC)_{ar}$. $\gamma(CH)_{ar}$	10a
854 w	854 w	853 w	855	4.20	862 vw	860 w	859 vw			862 vw		859 w				851 w	857 w			Ring def	
			840	5.69				850	3.42				854	0.01				858	3.64	$\Phi(CC)_{ar}$. $\gamma(CH)_{ar}$	10b
					817 w	821 w	826 m			827 w	826 w	825 m	817	16.62	819 w	819 m	821 m	803	27.70	$\beta_{sym}COO^{-}$	
			783	0.01				808	0.01				811	0.01						$\Phi(CC)_{ar}$. $\gamma(CH)_{ar}$	16a
753 m	751 m	761 s	741	88.65	765 m	758 m	769 vw	747	62.94	768 m	758 m	771 vw	749	59.36	751 m	751 m	765 vw	749	55.10	$\gamma(CH)_{ar}$	11
					727 m	731 m		738	120.98	727 w	726 m		725	68.78	718 m	719 m	728 vw	715	101.08	Ring def	
			707	31.19																βOH	
698 m	700 m	693 vw	703	74.41	704 m	702 m		699	20.24	701 m	702 m		700	16.98	701 m	700 m	703 vw	699	14.74	$\Phi(CC)_{ar}$. $\gamma(CH)_{ar}$	4
646 m	649 m	647 w	623	62.16	660 m	666 m	663 w	652	51.72	654 m	653 m	655 w	643	13.27	651 m	650 m	655 w	641	15.24	α(CCC)	6a
			632	55.27																βOH Ring d	
					626 m											627 m				α(CCC)	6b
582 w	588 w		591	0.01																γ(OH)	
			563	138.88																γ(OH)	
			543	0.01			543 vw	550	8.21	544 w			550	5.10				550	4.93	Ring def	
518 w	515 w				518 m					518 w		512 vw			500 w		499 w			$\gamma(CH)_{ar}$	
	496 w	487 vw			473 m			482	0.01			470 vw	487	0.01				481	0.01	$\Phi(CC)_{ar}$. $\gamma(CH)_{ar}$	16a
								493	2.99				481	9.62				477	9.31	$\beta_{as}COO^{-}$	
								425	5.74				427	4.50				427	3.76	$\Phi(CC)_{ar}$	16b
			449	14.24																Ring def	

Rubidium 2,6-pyridinedicarboxylate			Cesium 2,6-pyridinedicarboxylate			Assignments	
IR KBr	IR ATR	Raman	IR KBr	IR ATR	Raman		
		3135 w			3129 vw	$\nu(CH)_{ar}$	20a
		3079 vs			3073 s	$\nu(CH)_{ar}$	7b
		3000 vw			2994 vw	$\nu(CH)_{ar}$	13
1648 s	1650 w	1654 vw		1631 m	1636 w	$\nu_{as}COO^{-}$	
1612 vs	1607 s	1619 vw	1612 vs	1603 s		$\nu_{as}COO^{-}$	
1576 s	1575 m	1571 s	1575 s	1569 s	1569 s	$\nu(CC)_{ar}$, $\nu(CN)_{ar}$	8a
		1552 vw				$\nu(CC)_{ar}$, $\nu(CN)_{ar}$	8b
1432 m	1426 m	1432 s	1433 m	1423 m	1428 s	$\nu(CC)_{ar}$, $\nu(CN)_{ar}$, $\beta(CH)_{ar}$	19a
1378 vs	1371 vs	1390 vs	1379 vs	1365 vs	1386 vs	$\nu_{sym}COO^{-}$	
		1291 vw			1293 vw	$\nu(CC)_{ar}$, $\nu(CN)_{ar}$, $\beta(CH)_{ar}$	3
1266 w	1266 w		1266 w	1265 w		$\nu(CC)_{ar}$, $\nu(CN)_{ar}$, $\beta(CH)_{ar}$	15
1183 w	1185 w	1189 w	1184 w	1184 w	1185 vw	$\beta(CH)_{ar}$	
		1147 m	1147 w		1145 m	$\beta(CH)_{ar}$	18b
1119 vw			1117 w			$\beta(CH)_{ar}$	
1072 w	1069 w	1073 vw	1074 w	1069 w	1073 vw	$\beta(CH)_{ar}$	18a
1001 w	998 w	1004 vs	1000 w	997 w	1000 vs	$\Phi(CC)_{ar}$, $\gamma(CH)_{ar}$	17b

Table 2 *(continued)*

Rubidium 2,6-pyridinedicarboxylate			Cesium 2,6-pyridinedicarboxylate			Assignments	
IR KBr	IR ATR	Raman	IR KBr	IR ATR	Raman		
902 vw	902 w	904 vw	904 w	899 w	900 vw	$\Phi(CC)_{ar}$, $\gamma(CH)_{ar}$	10a
		855 vw			855 vw	$\Phi(CC)_{ar}$, $\gamma(CH)_{ar}$	10b
816 w	819 w	817 m	819 w	813 w	815 m	$\beta_{sym}COO^-$	
751 m	748 m	763 vw	752 m	751 m	759 vw	$\gamma(CH)_{ar}$	11
715 m	718 m		718 m	715 m	726 vw	$\alpha(CCC)$	
	701 w	703 vw				$\Phi(CC)_{ar}$, $\gamma(CH)_{ar}$	4
653 w	650 w	655 w	651 w	647 w	653 w	$\alpha(CCC)$	6a
617 w						$\alpha(CCC)$	6b
578 w			575 w		564 vw	Ring def	
501 w		499 vw	503 w		497 vw	$\Phi(CC)_{ar}$, $\gamma(CH)_{ar}$	16a

3.2. NMR spectra

Chemical shifts of the signals coming from protons in the ^{1}H NMR spectra of 2,3- and 2,6-PDA alkali metal salts take lower values than the corresponding ones for acids (Tables 3 and 4). An aromatic pyridine ring is disturbed, resulting in a change in the electron density around the protons of the aromatic ring. The values for the chemical shifts of aromatic protons labeled H3, H4 and H5 in the spectra of acid and its salts 2,6-PDA overlap to give a single band in the spectrum. For 2,3-PDA acid and its salts the three aromatic protons give its spectral image of three clearly separated signals. Decreases in proton chemical shifts for H4 and H5 in 2,3-PDA acid salts are small, and the decreases in proton chemical shifts for H3 are much larger and similar in size as those in 2,6-PDA salts.

The decisive factor influencing the electron charge distribution on the pyridine ring of 2,3-PDA and 2,6-PDA is the distribution of carboxyl groups linked to the ring. In the case of dipicolinic acid, the carboxyl groups are arranged symmetrically with respect to the nitrogen atom, with the consequence that the electronic charge around the carbon atoms is arranged symmetrically in the molecule. This can be observed as the equal values of the chemical shifts of carbons C2═C6 and C3═C5 in the ^{13}C NMR spectrum. In the case of 2,3-PDA, the carboxyl groups are asymmetrically attached to the aromatic ring, thereby the values for the chemical shifts of the carbons are asymmetrically distributed. Substitution of the carboxyl groups with an alkali metal atom induces the changes in the electronic charge distribution (implying the changes in the chemical shifts of the carbon atoms in the observed ^{13}C NMR spectra). Changes in the values of the chemical shifts for the carbon atoms in the spectra of 2,6-PDA salts occur in a symmetrical manner, i.e. the same increase in the chemical shifts of carbon C2 and C6, and the same decrease in chemical shifts for carbons C3 and C5 can be observed. In the case of 2,3-PDA salts, changes in the chemical shifts of the carbons (indicating the redistribution of the electronic charge in the molecules) are not symmetrical. In the series of salts of both acids the same direction of changes in chemical shifts is observed, i.e. an increase in the value of the signals for the carbon atoms C2 and C6 (decrease in electron density) and a decline in the value of the signals for C4 and C5 (increase in electron density) are found. Otherwise, for the C3 carbon atom of the 2,3-PDA salts an increase in chemical shifts relative to acid can be seen, whereas for the 2,6-PDA salts chemical shift values decrease. In conclusion, the electronic charge of the pyridine ring in the case of 2,6-PDA is distributed more evenly than in 2,3-PDA. Alkali metals perturb the electronic system to much higher degree, if the alkali metal atom is substituted to the carboxyl groups of 2,3-PDA than to those of 2,6-PDA.

3.3. Thermogravimetric study

Thermogravimetric studies of the 2,3- and 2,6-pyridinecarboxylate alkali metal salts (Tables 5 and 6) showed that the degrees of hydration of the 2,6-PDA alkali metal salts were very similar in the series (Li—Na—K—Rb—Cs). In the case of 2,3-PDA salts, the degree of hydration of each salt was also similar. The salts prior to the studies were dried for 24 h at 70 °C. Dehydration occurs in a

Table 3 Chemical shift values [ppm] in ^{1}H and ^{13}C NMR spectra of 2,3 PDA determined experimentally and theoretically by the GIAO/B3LYP/6-311++G** method.

		2,3-PDA acid	2,3-pyridinedicarboxylate				
			Lithium	Sodium	Potassium	Rubidium	Cesium
^{1}H NMR							
H4	Exp.	8.10	8.01	7.99	8.01	7.99	8.01
	Theoret.	8.54	8.58	7.61	8.67		
H5	Exp.	7.51	7.45	7.43	7.44	7.42	7.44
	Theoret.	7.37	6.99	7.05	6.75		
H6	Exp.	8.84	8.45	8.43	8.45	8.43	8.45
	Theoret.	8.75	8.72	8.42	8.57		
^{13}C NMR							
C2	Exp.	149.15	157.73	157.82	157.85	157.83	157.82
	Theoret.	160.91	170.96	157.71	172.17		
C3	Exp.	133.44	134.22	134.13	134.10	134.06	134.05
	Theoret.	127.23	125.82	147.23	129.53		
C4	Exp.	146.92	139.85	139.84	139.86	139.85	139.84
	Theoret.	144.98	145.27	137.13	144.88		
C5	Exp.	130.33	126.27	126.21	126.22	126.22	126.22
	Theoret.	127.31	123.32	127.60	121.55		
C6	Exp.	148.81	150.96	150.95	150.98	150.97	150.97
	Theoret.	157.69	159.61	150.62	157.44		
C7	Exp.	170.05	177.74	177.77	177.81	177.80	176.84
	Theoret.	172.39	184.07	187.42	183.28		
C8	Exp.	167.24	176.96	176.90	176.90	176.87	177.74
	Theoret.	169.52	190.97	185.05	184.10		

Table 4 Chemical shift values [ppm] in ^{1}H and ^{13}C NMR spectra of 2,6 PDA determined experimentally and theoretically by the GIAO/B3LYP/6-311++G** method.

		2,6-PDA acid	2,6-pyridinedicarboxylate				
			Lithium	Sodium	Potassium	Rubidium	Cesium
^{1}H NMR							
H3	Exp.	8.41	8.01	7.99	8.00	7.98	7.97
	Theoret.	8.32	8.50	8.45	8.46		
H4	Exp.	8.41	8.01	7.99	8.00	7.98	7.97
	Theoret.	7.83	7.67	7.52	7.48		
H5	Exp.	8.41	8.01	7.99	8.00	7.98	7.97
	Theoret.	8.32	8.50	8.45	8.46		
^{13}C NMR							
C2	Exp.	149.97	155.16	155.39	155.49	155.48	155.49
	Theoret.	153.03	157.16	158.89	159.99		
C3	Exp.	145.59	141.50	141.23	141.23	141.21	141.27
	Theoret.	133.49	131.71	130.77	129.56		
C4	Exp.	130.95	127.80	127.72	127.75	127.72	127.72
	Theoret.	141.09	138.85	137.79	137.05		
C5	Exp.	145.59	141.50	141.23	141.23	141.21	141.27
	Theoret.	133.49	131.71	130.77	129.56		
C6	Exp.	149.97	155.16	155.39	155.49	155.48	155.49
	Theoret.	153.03	157.16	158.89	159.99		
C7	Exp.	168.60	175.54	175.73	175.77	175.78	175.78
	Theoret.	165.05	187.23	181.45	181.53		
C8	Exp.	168.60	175.54	175.73	175.77	175.78	175.78
	Theoret.	165.05	187.23	181.45	181.53		

Please cite this article in press as: Świderski, G. et al., Spectroscopic (IR, Raman, NMR), thermal and theoretical (DFT) study of alkali metal dipicolinates (2,6) and quinolinates (2,3). Arabian Journal of Chemistry (2016), http://dx.doi.org/10.1016/j.arabjc.2016.06.011

Table 5 Thermogravimetric analysis for lithium, sodium, potassium, rubidium and cesium 2,3-pyridinedicarboxylates.

Compound	Range of decomposition	Weight loss (%)		Product decomposition
		Calc.	Found	
$Li_2L{\cdot}0{,}5H_2O$	140–210	4.74	4.80	Li_2L
	370–550	–	31.0	$Li_2CO_3 + C_{org}$
	550–850	61.11	62.0	Li_2CO_3
$Na_2L{\cdot}H_2O$	140–160	7.78	7.75	Na_2L
	410–490	–	25.0	$Na_2CO_3 + C_{org}$
	490–740	54.11	54.0	Na_2CO_3
$K_2L{\cdot}0{,}5H_2O$	130–210	3.54	3.6	K_2L
	380–510	–	22	$K_2CO_3 + C_{org}$
	510–750	45.6	45.0	K_2CO_3
	750 <	–	–	K_2O
$Rb_2L{\cdot}0{,}75H_2O$	130–210	3.84	3.6	Rb_2L
	400–480	–	15	$Rb_2CO_3 + C_{org}$
	500–830	53.25	53.0	Rb_2CO_3
	830 <	–	–	Rb_2O
$Cs_2L{\cdot}0{,}5H_2O$	110–150	2.04	2.0	Cs_2L
	390–490	–	10.0	$Cs_2CO_3 + C_{org}$
	490 <	–	–	Cs_2O

Table 6 Thermogravimetric analysis for lithium, sodium, potassium, rubidium and cesium 2,6-pyridinedicarboxylates.

Compound	Range of decomposition	Weight loss (%)		Product decomposition
		Calc.	Found	
$Li_2L{\cdot}0{,}75H_2O$	100–210	6.94	7.2	Li_2L
	450–510	–	20.0	$Li_2CO_3 + C_{org}$
	510–890	84.3	85.0	Li_2O
$Na_2L{\cdot}0{,}75H_2O$	100–150	5.95	5.6	Na_2L
	460–510	–	22.0	$Na_2CO_3 + C_{org}$
	510–850	52.1	52.0	Na_2CO_3
$K_2L{\cdot}0{,}75H_2O$	100–170	5.21	5.0	K_2L
	450–490	–	21.0	$K_2CO_3 + C_{org}$
	490–890	–	58.0	$K_2CO_3 + K_2O$
$Rb_2L{\cdot}0{,}5H_2O$	100–210	2.59	2.8	Rb_2L
	430–490		16.0	$Rb_2CO_3 + C_{org}$
	> 850	–	–	Rb_2O
$Cs_2L{\cdot}0{,}75H_2O$	100–210	3.02	3.0	Cs_2L
	410–480	–	10.0	$Cs_2CO_3 + C_{org}$
	> 830	–	–	Cs_2O

single step for the salts tested (all hydrated salts). For the 2,6-PDA salts the dehydration process begins at 100 °C. Sodium and potassium salts of 2,6-PDA loose water in the temperature range of 100–210 °C, and all other salts in the range of 100–150 °C. The process for the dehydration of the 2,3-PDA salts starts at slightly higher temperatures (above 130 °C). After dehydration, in subsequent steps the process of decomposition of the tested compounds occurs. Both acids are degraded completely in a one-step process of decomposition at about 250 °C. Studies on the decomposition of salts in the range of 70–890 °C showed that the decomposition proceeds via formation of alkali metal carbonates and in a later step in the case of certain salts, to alkali metal oxides. In the first step in a temperature range from ca 370 to 500 °C beside carbonates some residues of organic carbon are found as well that are formed during the decomposition of the aromatic ring. This can be seen as a pitch curve on TG and DTA graphs (Fig. 3). In a further step of the decomposition process the organic carbon residues are oxidized to carbon dioxide and a product in the form of carbonate is formed. In the case of sodium salts the produced carbonates are stable in a range of temperatures, while for the other salts a decomposition of carbonates to the oxides of alkali metals occurs. Comparing the curves illustrating the thermal decomposition of the alkali metal salts of the two studied acids (Fig. 3) one can observe that salts of 2,6-PDA are dehydrated at a slightly lower temperature than the salts of 2,3-PDA. In contrast, the decomposition of the aromatic ring occurs at a slightly lower temperature in the case of 2,3-PDA salts than for those of 2,6-PDA. Based on the decomposition curve, it can be concluded that the 2,3-pyridinedicarboxylates are thermally less stable than the 2,6-pyridinedicarboxylates of the alkali metals.

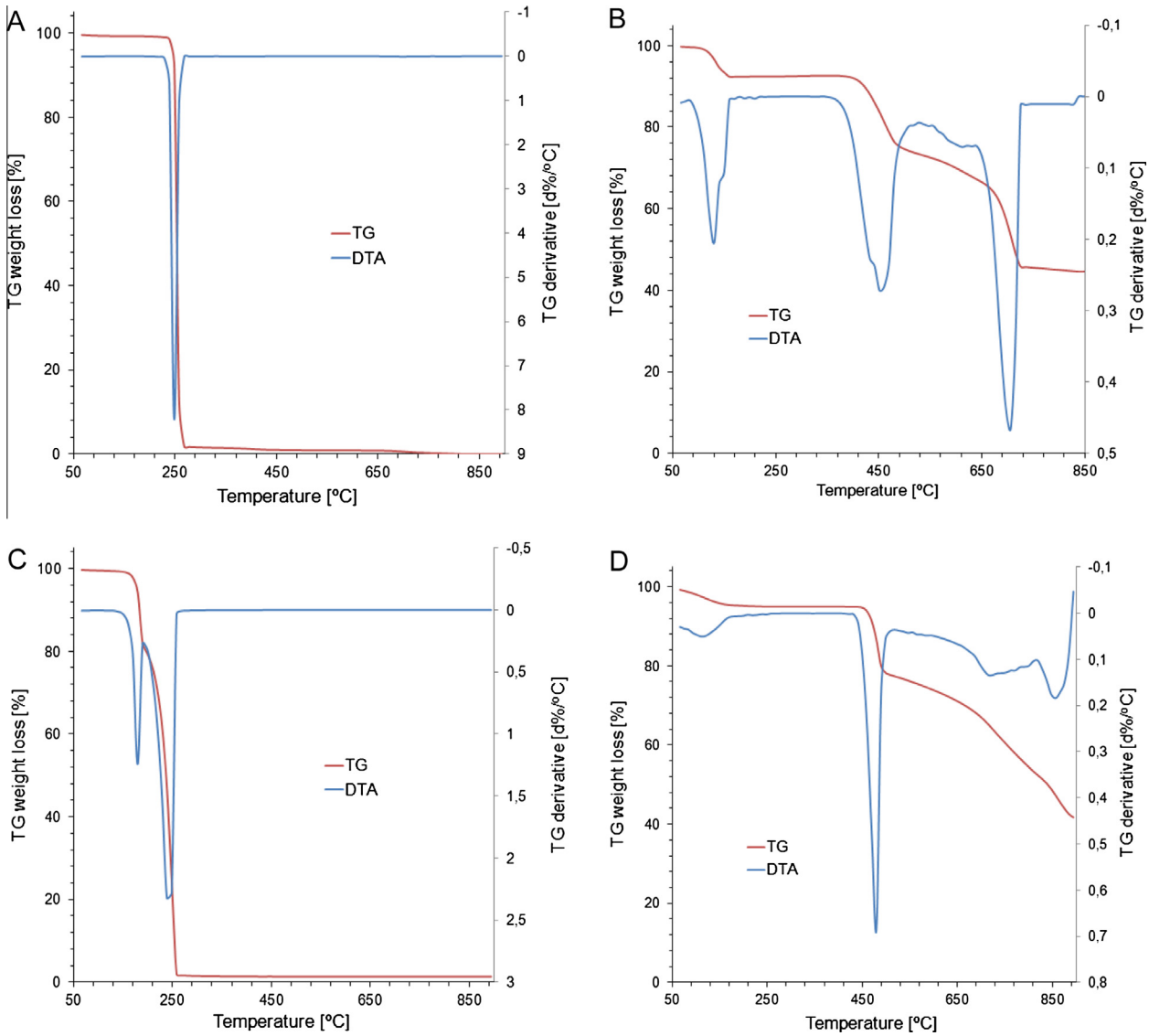

Figure 3 TG/DTA curves of 2,3-pyridinedicarboxylic acid (A) and sodium salts (B), 2,6-pyridinedicarboxylic acid (C) and sodium salts (D).

4. Conclusions

It was observed that in the IR and Raman spectra of 2,3-PDA alkali metal salts there disappear more bands that are initially present in the ligand than in the case of 2,6-PDA salts. In addition, in the salts of 2,6-PDA more new bands appear than in the case of 2,3-PDA salts, as compared to the respective ligand.

Changes in the spectra of the alkali metal salt of the acid with respect to the acid spectra are related to the effects of metal on the electron charge distribution of the aromatic ring of the ligand. The alkali metals destabilize the electronic system, and the effect is greater for 2,3-pyridinecarboxylates. In the case of 2,6-PDA acid molecules electron charge distribution in the aromatic ring is symmetrical with respect to the nitrogen atom, due to the symmetrical position of the carboxyl groups, what is indicated by chemical shift values in ^{1}H NMR and ^{13}C NMR spectra. Alkali metal substitution in the carboxyl group of this acid causes changes in the distribution of electron charge (seen as changes in chemical shifts), and the symmetry of the charge distribution in the aromatic ring is retained with respect to the heteroatom. When the carboxylic groups take an asymmetric position relative to the heteroatom in the 2,3-PDA ring, the asymmetric distribution of electron charge is observed. An alkali metal atom substitution in the carboxyl group induces an increase of an asymmetric charge distribution in the aromatic ring – a perturbation of the charge distribution increases in the tested series of salts in the order Li → Na → K → Rb → Cs. Based on the decomposition curve it can be concluded that the 2,3-pyridinedicarboxylates of alkali metals are thermally less stable compounds than the 2,6-pyridinedicarboxylates of the alkali metals.

Acknowledgements

This work was supported by Bialystok University of Technology in the frame of funding for statutory research (no. S/WBiIŚ/1/2012).
Thermogravimetric study was performed at the Center of Synthesis and Analysis BioNanoTechno of the University of Bialystok. The equipment in the Center of Synthesis and Analysis BioNanoTechno of University of Bialystok was funded by the EU, project: POPW.01.03.00–20–034/09–00.

Appendix A. Supplementary material

Supplementary data associated with this article can be found, in the online version, at http://dx.doi.org/10.1016/j.arabjc.2016.06.011.

References

Bruyn, R.P.M., Stoof, J.C., 1990. The quinolinic acid hypothesis in Huntington's chorea. J. Neurol. Sci. 95 (1), 29–38.

Chen, Y., Brew, B.J., Guillemin, G.J., 2011. Characterization of the kynurenine pathway in NSC-34 cell line: implications for amyotrophic lateral sclerosis. J. Neurochem. 118 (5), 816–825.

Chen, Y., Stankovic, R., Cullen, K.M., Meininger, V., Garner, B., Coggan, S., Grant, R., Brew, B.J., Guillemin, G.J., 2010. The kynurenine pathway and inflammation in amyotrophic lateral sclerosis. Neurotox. Res. 18 (2), 132–142.

Frisch, M., Trucks, G.W., Schlegel, H.B., Scuseria, G.E., Robb, M.A., Cheeseman, J.R., Scalmani, G., Barone, V., Mennucci, B., Petersson, G.A., 2009. Gaussian 09, revision A. 02. Gaussian, Inc., Wallingford, CT, pp. 227–238, 19.

Guillemin, G.J., Brew, B.J., 2002. Implications of the kynurenine pathway and quinolinic acid in Alzheimer's disease. Redox Rep. 7, 199–206.

Guillemin, G.J., Brew, B.J., Noonan, C.E., Takikawa, O., Cullen, K. M., 2005. Indoleamine 2,3 dioxygenase and quinolinic acid Immunoreactivity in Alzheimer's disease hippocampus. Neuropathol. Appl. Neurobiol. 31 (4), 395–404.

Guillemin, G.J., Williams, K.R., Smith, D.G., Smythe, G.A., Croitoru-Lamoury, J., Brew, B.J., 2003. Quinolinic acid in the pathogenesis of Alzheimer's disease. Adv. Exp. Med. Biol. 527, 167–176.

Hartai, Z., Klivenyi, P., Janaky, T., Penke, B., Dux, L., Vecsei, L., 2005. Kynurenine metabolism in multiple sclerosis. Acta Neurol. Scand. 112 (2), 93–96.

Heyes, M.P., Saito, K., Crowley, J.S., Davis, L.E., Demitrack, M.A., Der, M., Dilling, L.A., Elia, J., Kruesi, M.J., Lackner, A., et al, 1992. Quinolinic acid and kynurenine pathway metabolism in inflammatory and non-inflammatory neurological disease. Brain 115, 1249–1273.

Kalinowska, M., Borawska, M., Świsłocka, R., Piekut, J., Lewandowski, W., 2007. Spectroscopic (IR, Raman, UV, ^{1}H and ^{13}C NMR) and microbiological studies of Fe(III), Ni(II), Cu(II), Zn(II) and Ag(I) picolinates. J. Mol. Struct. 834, 419–425.

Karabacak, M., Sinha, L., Prasad, O., Bilgili, S., Sachan, A.K., Asiri, A.M., Atac, A., 2015. Spectral investigation and theoretical study of zwitterionic and neutral forms of quinolinic acid. J. Mol. Struct. 1095, 100–111.

Koczoń, P., Piekut, J., Borawska, M., Świsłocka, R., Lewandowski, W., 2006. Vibrational and microbiological study on alkaline metal picolinates and o-iodobenzoates. Anal. Bioanal. Chem. 384 (1), 302–308.

Kubicova, L., Hadacek, F., Weckwerth, W., Chobot, V., 2015. Effects of endogenous neurotoxin quinolinic acid on reactive oxygen species production by Fenton reaction catalyzed by iron or copper. J. Organomet. Chem. 782, 111–115.

Lewandowski, W., Świderski, G., Świslocka, R., Wojtulewski, S., Koczoń, P., 2005. Spectroscopic (Raman, FT-IR and NMR) and theoretical study of alkali metal picolinates. J. Phys. Org. Chem. 18 (9), 918–928.

Lim, C.K., Brew, B.J., Sundaram, G., Guillemin, G.J., 2010. Understanding the roles of the kynurenine pathway in multiple sclerosis progression. Int. J. Tryptophan Res. 3, 157–167.

McCann, K., Laane, J., 2008. Raman and infrared spectra and theoretical calculations of dipicolinic acid, dinicotinic acid, and their dianions. J. Mol. Struct. 890 (1), 346–358.

Pérez-De La Cruz, V., Königsberg, M., Santamaría, A., 2007. Kynurenine pathway and disease: an overview. CNS Neurol. Disord. Drug Targets 6, 398–410.

Powell, J.F., Strange, R.E., 1953. Biochemical changes occurring during the germination of bacterial spores. Biochem. J. 54 (2), 205–209.

Rahman, A., Ting, K., Cullen, K.M., Braidy, N., Brew, B.J., Guillemin, G.J., 2009. The excitotoxin quinolinic acid induces tau phosphorylation in human neurons. PLoS One 4 (7), e6344.

Rode, J.E., Dobrowolski, J.C., Jamróz, M.H., Borowiak, M.A., 2001. Theoretical IR, Raman and NMR spectra of 1, 2-and 1, 3-dimethylenecyclobutane. Vib. Spectrosc. 25, 133–149.

Slieman, T.A., Nicholson, W.L., 2001. Role of dipicolinic acid in survival of bacillus subtilis spores exposed to artificial and solar UV radiation. Appl. Environ. Microbial. 67 (3), 1274–1279.

Stoy, N., Mackay, G.M., Forrest, C.M., Christofides, J., Egerton, M., Stone, T.W., Darlington, L.G., 2005. Tryptophan metabolism and oxidative stress in patients with Huntington's disease. J. Neurochem. 93 (3), 611–623.

Świderski, G., Kalinowska, M., Wojtulewski, S., Lewandowski, W., 2006. Experimental (FT-IR, FT-Raman, 1 H NMR) and theoretical study of magnesium, calcium, strontium, and barium picolinates. Spectrochim. Acta Part A 64 (1), 24–33.

Varsanyi, G., 1973. In: Vibrational Spectra of 700 Benzene Derivatives, vol. I–II. Academic Kiaclo, Budapest.

Zinger, A., Barcia, C., Herrero, M.T., Guillemin, G.J., 2011. The involvement of neuroinflammation and kynurenine pathway in Parkinson's disease. Parkinson's Dis. 2011.